

Optical Engineering

OpticalEngineering.SPIEDigitalLibrary.org

Easy conductive calibration method for binocular vision system based on collinear image transformation

Enkun Cui
YanJie Wang
Tao Zhang
Nan Di
YanHe Yin
Pei Wu
HongHai Sun

SPIE.

Enkun Cui, YanJie Wang, Tao Zhang, Nan Di, YanHe Yin, Pei Wu, HongHai Sun, "Easy conductive calibration method for binocular vision system based on collinear image transformation," *Opt. Eng.* **56**(10), 103106 (2017), doi: 10.1117/1.OE.56.10.103106.

Easy conductive calibration method for binocular vision system based on collinear image transformation

Enkun Cui,^{a,b,*} YanJie Wang,^b Tao Zhang,^b Nan Di,^b YanHe Yin,^{a,b} Pei Wu,^{a,b} and HongHai Sun^b

^aUniversity of Chinese Academy of Sciences, Beijing, China

^bChinese Academy of Sciences, Changchun Institute of Optic, Fine Mechanics and Physics, Changchun, Jilin, China

Abstract. This paper presents an effective technique to calibrate the binocular system. A collinear geometry transformation is derived and introduced into the calibration process. First, we construct a virtual binocular system with every two point pair in the same image, and then an analytic method based on the virtual binocular system is proposed to calculate the internal and external parameters of left and right cameras. The structure parameters are solved from the calibrated extrinsic parameters of each camera. All the parameters of the binocular system are calculated with only one image pair. Furthermore, an iterative refinement by minimizing the metric distance error between the reconstructed point and the real point in a three-dimensional measurement coordinate system is applied to enhance the calibration accuracy. Simulations and real experiments have been carried out. The calibration accuracy is compared with the traditional calibration method. The results show that the proposed calibration methods are efficient in improving the calibration accuracy and simply equipped. © 2017 Society of Photo-Optical Instrumentation Engineers (SPIE) [DOI: 10.1117/1.OE.56.10.103106]

Keywords: machine vision; calibration; vision binocular.

Paper 170984 received Jul. 5, 2017; accepted for publication Sep. 22, 2017; published online Oct. 16, 2017.

1 Introduction

The binocular stereo vision system is a three-dimensional (3-D), noncontact, real-time, and high-precision measurement technology.¹ It is widely used in geometric measurement, motion measurement, and other measurement applications. Concerning its measurement accuracy, one of the most important problems surrounding the binocular vision system is the accuracy of the calibration.^{2–5} Considering stereo vision system calibration, usually the whole process is divided into two steps. At the first stage, the single camera is calibrated to obtain the intrinsic parameters, extrinsic parameters, and distortion coefficients.^{6–9} After that, the structure parameters that represent the relative position and rotation of the two cameras are determined. Many methods have been put forward to calibrate the binocular system. For example, Ref. 4 introduces an optimization method by minimizing the metric distance between actual and computed object points in a 3-D coordinate system. The computed object point is calculated by the intersection of target plane and the corresponding ray. In Ref. 5, linear method and nonlinear optimization are combined to estimate the structure parameters of a binocular vision sensor relying on vanishing feature constraints and spacing constraints of parallel lines. Usually, most calibration methods are based on the fact that target position is determined. As we know, it is difficult to obtain the accurate position between the target and the camera. In addition, some calibration methods need high-precision movement. Hartley¹⁰ proposed a calibration method based on rotation. This method requires at least three images with different orientations of the same camera at the same point in space to analyze point matching between images; furthermore, pure rotation is required in this method, which is difficult to ensure.¹¹ Self-calibration uses constraints

among the system parameters to calibrate cameras,^{12–14} which makes it possible to calibrate the system using unknown scenes and motions.

Nowadays, the genetic algorithms¹⁵ based on the structural light can calibrate the microscope vision parameters without external references, so the errors of external references are not introduced to the calibration process. In this paper, a collinear geometric imaging transformation is presented. We propose a binocular system calibration method based on this transformation. The proposed method calculates all the parameters by analytic algorithms and also without any external references. During the analytic algorithms, we divide the calibration process of the binocular vision system into two parts: one part is to determine the internal and external parameters and the distortion coefficients of left and right cameras. The other part is to determine the structure parameters, which describe the spatial relationship between the two cameras. In addition, employing the image process skill to extract observed points from images introduces the extraction noise absolutely. The camera parameters are often obtained through iteration with the constraint of minimizing an objective function.^{4,16} So after the parameters are calculated with an analytic method, a nonlinear optimization process is employed to refine all the parameters. The proposed method is easy executive without any requirement of special movement or calibration target position information. The rest of the paper is organized to explain the proposed calibration method by the following direction: in Sec. 2, the related work on geometric relationship of binocular system is analyzed, and the collinear geometry transformation is explained. Next, the detailed procedure of the proposed calibration method is described in Sec. 3. In Sec. 4, computer simulation experiment and real data experiment are carried out to evaluate our

*Address all correspondence to: Enkun Cui, E-mail: cuiek08@163.com

method. The result of our experiment verifies accuracy of the proposed method. The paper ends with some concluding remarks in Sec. 5.

2 Related Research

2.1 Geometry of Binocular Vision System

The geometry of the binocular system is shown in Fig. 1. O_l and O_r are the optical centers of the left and right cameras, respectively. For the same view of a 3-D field caught by left camera and right camera, given a point \tilde{m}_l in the left image, its corresponding point \tilde{m}_r in the right image, algebraically the relationship between a 3-D point M_w and its image projections in the left and right cameras is written as follows:

$$\lambda_l \tilde{m}_l = A_l(R_l|T_l)\tilde{M}_w, \quad \lambda_r \tilde{m}_r = A_r(R_r|T_r)\tilde{M}_w, \quad (1)$$

$$A_l = \begin{bmatrix} f_{xl} & 0 & u_{0l} \\ 0 & f_{yl} & v_{0l} \\ 0 & 0 & 1 \end{bmatrix}, A_r = \begin{bmatrix} f_{xr} & 0 & u_{0r} \\ 0 & f_{yr} & v_{0r} \\ 0 & 0 & 1 \end{bmatrix},$$

where (R_l, T_l) and (R_r, T_r) , called the extrinsic parameters, are the rotation and translation, which relate to the world coordinate system to the camera coordinate system, A_l and A_r are the intrinsic camera matrices consisting of the following parameters: (f_{xl}, f_{yl}) and (f_{xr}, f_{yr}) are the effective focal length and (u_{0l}, v_{0l}) and (u_{0r}, v_{0r}) are the coordinates of the principal point. \tilde{m} and \tilde{M}_w are the homogeneous coordinates of the image coordinate and object point coordinate M_w in the world coordinate system, respectively; λ_l and λ_r are the arbitrary scale factors. The structure parameters (R, T) can be solved from the calibrated extrinsic parameters of each camera

$$R = R_r R_l^{-1}, T = T_r - R_r R_l^{-1} T_l. \quad (2)$$

The main aim of the binocular calibration procedure is to determine the parameters to perform 3-D measurements. If the stereo correspondence between two image points has been established, then the calibrated camera parameters can be applied to reconstruct the 3-D space coordinate by triangulation.

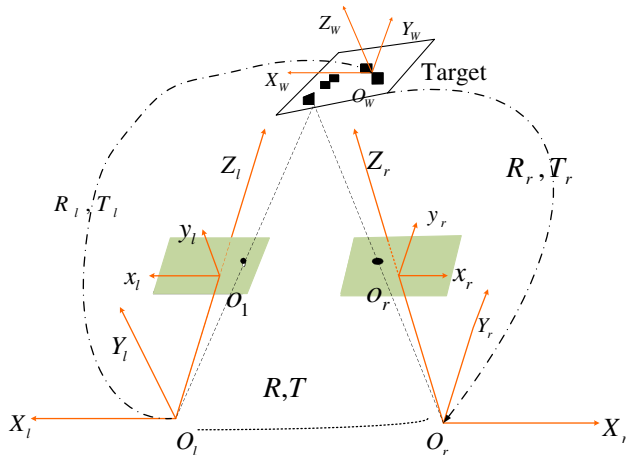


Fig. 1 The complete imaging geometrical model of binocular vision system.

2.2 Collinear Geometry

To explain the collinear geometry, we construct a virtual binocular system. For the virtual binocular system, the internal camera parameters are the same as that in Fig. 1. The rotation matrices R_l and R_r are the same as that in Fig. 1. The only difference is that the translation vectors T_r and T_l are zero. The geometry relationship is shown in Fig. 2, $O_w X_w Y_w Z_w$ is the coordinate system of the calibration target, i.e., the world coordinate system. $O_l X_l Y_l Z_l$ and $O_r X_r Y_r Z_r$ are the left and right camera coordinate systems, respectively. The two planes are the right and left image planes, respectively. A point M is imaged in the left and right cameras, denoted as $\tilde{m}_{1l} = (U_{1l}, V_{1l}, 1)$ or $\tilde{m}_{1r} = (U_{1r}, V_{1r}, 1)$. The virtual image of P can be written as follows:

$$\lambda_1 \tilde{m}_1 = A \hat{M}, \quad \hat{M} = R_n M_w, \quad \text{and} \quad \tilde{m}_1 = (U_1, V_1, 1), \quad (3)$$

where n represents l or r . It can be found that the optical central of the two cameras coincides. \tilde{m}_{1l} and \tilde{m}_{1r} lie in the same line (the line connecting the object point and optical center). The translation vector between the world coordinate system and camera coordinate system is zero, the collinear geometry relationship in the right camera coordinate system is expressed as follows:

$$\begin{pmatrix} x_{lr} \\ y_{lr} \\ z_{lr} \end{pmatrix} = R \begin{pmatrix} U_{1l} \\ V_{1l} \\ 1 \end{pmatrix}, \quad (4)$$

$$\frac{x_{lr} - U_{1r}}{U_{1r}} = \frac{y_{lr} - V_{1r}}{V_{1r}} = \frac{z_{lr} - 1}{1}, \quad (5)$$

where $m_{lr} = (x_{lr}, y_{lr}, z_{lr})$ denotes the coordinate of \tilde{m}_{1l} in the right camera coordinate system. We assume the real image captured by the binocular system is $m(U, V)$, which is explained as Eq. (1). Compare the two projection equations [Eqs. (1) and (3)], the relationship between the virtual and the real images can be obtained

$$U_{1n} = a_u U_n - b_u, \quad V_{1n} = a_v V_n - b_v, \quad (6)$$

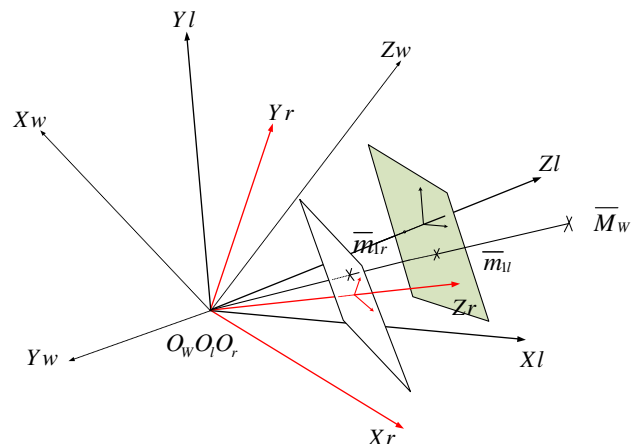


Fig. 2 The complete imaging geometrical model of centroid coordinate systems.

$$\begin{aligned} a_u &= 1 + \frac{t_{3n}}{z_1}, \\ a_v &= 1 + \frac{t_{3n}}{z_1}, \\ b_u &= \frac{f_{xn}t_{1n} + u_{0n}t_{3n}}{z_1}, \quad \text{and} \\ b_v &= \frac{f_{yn}t_{2n} + v_{0n}t_{3n}}{z_1}, \end{aligned}$$

where t_{in} is the i 'th element of T_n and z_1 is the z coordinate of \hat{M} .

3 Analytic Calibration Methods Based on Collinear Geometry

3.1 Compute Distortion Coefficients

A camera usually exhibits significant lens distortion,^{2,9,17} it is likely that the distortion function is totally dominated by the radial components and especially dominated by the first term. We choose the division model for radial distortion as follow:

$$m_u - e = \frac{(m_d - e)}{1 + k_1 r_d^2 + k_2 r_d^4 + \dots}, \quad (7)$$

where k_1, k_2, \dots are the distortion coefficients, $e = (du, dv, 1)^T$ is the homogeneous coordinate of the center of distortion (COD), and r_d is the pixel radius to e . In this paper, we only consider the first two terms of radial distortion. We adopt the method proposed in Ref. 18 to accurately estimate the position of COD and solve the distortion coefficients. Calculate the undistorted image points m_d from the detected counterpart m_u according to the distortion coefficients k_1, k_2 , COD [Eq. (7)]

$$m_u(\bar{U}, \bar{V}) \rightarrow m_d(U, V). \quad (8)$$

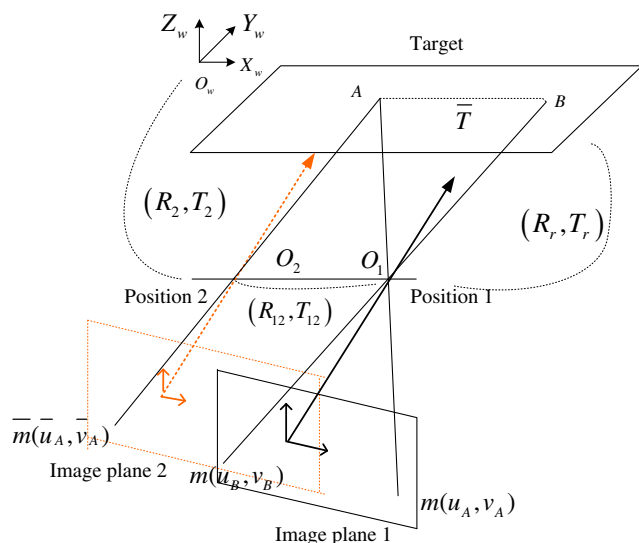


Fig. 3 The transformation of two points in the same image.

3.2 Single Camera Calibration

To calculate the exact solution of a single camera's parameters, we make a structure transform. We take the right camera of the binocular system as an example. As shown in Fig. 3, right camera is in position 1. The structure transform is based on the assumption that there is another virtual camera in position 2. The virtual camera's internal parameters are the same as the right camera's. Upon this assumption, the right camera and the virtual camera constitute a virtual binocular system. $A[M_A(x_A, y_A, z_A)]$ and $B[M_B(x_B, y_B, z_B)]$ are the two points on the target, $\tilde{m}_A(U_A, V_A, 1)$ and $\tilde{m}_B(U_B, V_B, 1)$ are images of A and B captured using the right camera. Let $\bar{T} = M_B - M_A$ represents the vector AB in the world coordinate system. If camera in position 2 satisfies the follow relationship: The location of A' image in the image plane of camera 2 is the same as that of B' image in the image plane of camera 1, namely the coordinate of A in the coordinate system of camera 2 is equal to the coordinate of B in the coordinate system of camera 1. Then, we can consider the image of B in camera 1 as the image of A on camera 2. In this way, we get the images of A in left and right cameras of the virtual binocular system. Assuming (R_r, T_r) and (R_2, T_2) relate world coordinate system to camera coordinate system in position 1 and position 2, respectively. The requirement for the virtual binocular system is as follows:

$$\begin{pmatrix} R_2 & T_2 \\ 0 & 1 \end{pmatrix} \begin{pmatrix} M_A \\ 1 \end{pmatrix} = \begin{pmatrix} R_r & T_r \\ 0 & 1 \end{pmatrix} \begin{pmatrix} M_B \\ 1 \end{pmatrix}. \quad (9)$$

The right part of Eq. (9) can be written in the following form:

$$\begin{pmatrix} R_r & T_r \\ 0 & 1 \end{pmatrix} \begin{pmatrix} M_A + \bar{T} \\ 1 \end{pmatrix} = \begin{pmatrix} R_r & T_r \\ 0 & 1 \end{pmatrix} \begin{pmatrix} E & \bar{T} \\ 0 & 1 \end{pmatrix} \begin{pmatrix} M_A \\ 1 \end{pmatrix}. \quad (10)$$

Then, we can get the following equations:

$$R_2 = R_r, T_2 = R_r \bar{T} + T_r, \quad (11)$$

$$R_{12} = I, T_{12} = R_r \bar{T}, \quad (12)$$

where R_{12} and T_{12} are the structure parameters of the virtual binocular system relating the camera in position 2 to the camera in position 1. Now, the images of two points in the same picture are transformed to images of the same point in two pictures. Then, $\tilde{m}_A(U_A, V_A, 1)$ and $\tilde{m}_B(U_B, V_B, 1)$ are seen as the images of A captured by the binocular system.

Now, we calculate the internal and external parameters A_r and (R_r, T_r) based on the above virtual binocular system. \tilde{m}_A and \tilde{m}_B can be transformed to the virtual images with Eq. (6), denoted as $\tilde{m}_{A1}(U_{A1}, V_{A1}, 1)$ and $\tilde{m}_{B1}(U_{B1}, V_{B1}, 1)$, respectively. As the extrinsic rotation matrix in position 1 is the same as in position 2 ($R_2 = R_r$), we note that \tilde{m}_{A1} equals to \tilde{m}_{B1} . Then, the following relationship can be obtained:

$$(\bar{r}_{3r} M_A + t_{3r}) \begin{pmatrix} U_A - U_B \\ V_A - V_B \end{pmatrix} = \begin{pmatrix} -f_x & 0 & U_B - u_0 \\ 0 & -f_y & V_B - v_0 \end{pmatrix} R_r \bar{T}, \quad (13)$$

where \bar{r}_{ir} represents the i 'th row of R_r . Equation (13) is a nonlinear equation of internal and external camera parameters.

To make this function work well, first we choose two image pairs $[M_A(x_A, y_A, z_A), M_B(x_B, y_B, z_B)]$ and $[\bar{M}_A(\bar{x}_A, \bar{y}_A, \bar{z}_A), \bar{M}_B(\bar{x}_B, \bar{y}_B, \bar{z}_B)]$. If the two image pairs satisfy the condition $[\bar{T} = \bar{T}_1 = T \cdot [\bar{T} = (x_B - x_A, y_B - y_A, z_B - z_A)]$ and $\bar{T}_1 = (\bar{x}_B - \bar{x}_A, \bar{y}_B - \bar{y}_A, \bar{z}_B - \bar{z}_A)$, take the two image pairs into Eq. (13), respectively, and two equations are obtained. Two equations minus each other, then the following function is obtained:

$$\bar{r}_{3r}[M_A(U_A - U_B) - \bar{M}_A(\bar{U}_A - \bar{U}_B) - \bar{T}(U_B - \bar{U}_B)] + t_{3r}[(U_A - U_B) - (\bar{U}_A - \bar{U}_B)] = 0. \quad (14)$$

We can see that the only variables left in this equation are \bar{r}_{3r} and t_{3r} . This is a linear function about \bar{r}_{3r} and t_{3r} . The equation about $(V_A, V_B, \bar{V}_A, \bar{V}_B)$ can also be obtained. Note that we cannot calculate \bar{r}_{3l} and t_{3l} directly. Instead, we compute \bar{r}_{3r}/t_{3r} . Then, the elements of \bar{r}_{3r} and t_{3r} can be calculated with $\bar{r}_{31r}^2 + \bar{r}_{32r}^2 + \bar{r}_{33r}^2 = 1$, \bar{r}_{ij} is the j 'th element in the i 'th row of R_r . This means noncoplanar target is needed in this method.

To compute the rest parameters, we replace \bar{T} in Eq. (13) with $M_B - M_A$, then Eq. (13) can be rewritten in the following form:

$$\begin{pmatrix} x_b - x_a & y_b - y_a & z_b - z_a \end{pmatrix} P_{IX1} = \bar{r}_{3r}(M_B U_B - M_A U_A) + t_{3r}(U_B - U_A) \quad (15)$$

$$\begin{pmatrix} x_b - x_a & y_b - y_a & z_b - z_a \end{pmatrix} P_{IX2} = \bar{r}_{3r}(M_B V_B - M_A V_A) + t_{3r}(V_B - V_A), \quad (16)$$

$$P_{IX1} = \begin{pmatrix} f_{xr}r_{11r} + u_{0r}r_{31r} \\ f_{xr}r_{12r} + u_{0r}r_{32r} \\ f_{xr}r_{13r} + u_{0r}r_{33r} \end{pmatrix},$$

$$P_{IX2} = \begin{pmatrix} f_{yr}r_{21r} + v_{0r}r_{31r} \\ f_{yr}r_{22r} + v_{0r}r_{32r} \\ f_{yr}r_{23r} + v_{0r}r_{33r} \end{pmatrix}.$$

Since \bar{r}_{3r} and t_{3r} have been calculated with Eq. (14), the right parts of Eqs. (15) and (16) are known. Only three point pairs are needed to calculate the value of P_{IX1} and P_{IX2} . After the values of P_{IX1} and P_{IX2} are obtained, we can calculate $\bar{r}_{1r}, \bar{r}_{2r}, f_{xr}, f_{yr}, u_{0r}$, and v_{0r} with the following equations:

$$\bar{r}_{1r} \times \bar{r}_{2r} = \bar{r}_{3r} \quad (17)$$

$$r_{11r}^2 + r_{12r}^2 + r_{13r}^2 = 1 \quad \text{and} \quad r_{21r}^2 + r_{22r}^2 + r_{23r}^2 = 1. \quad (18)$$

Then, t_{1r} and t_{2r} can be easily obtained. Now all the internal and external parameters are obtained with only one picture. The only requirement is aware of the points arrange information in the target. The left camera can also be calibrated in the same way above. The structure parameters can be solved from the calibrated extrinsic parameters of each camera using Eq. (2).

Since no iterations are required, the proposed camera calibration method is computationally fast. All the parameters of the binocular system can be obtained with only one image pair (the left and right images). However, the proposed method also has some limitations. It requires a noncoplanar target. Of course, an iterative refinement of the results would

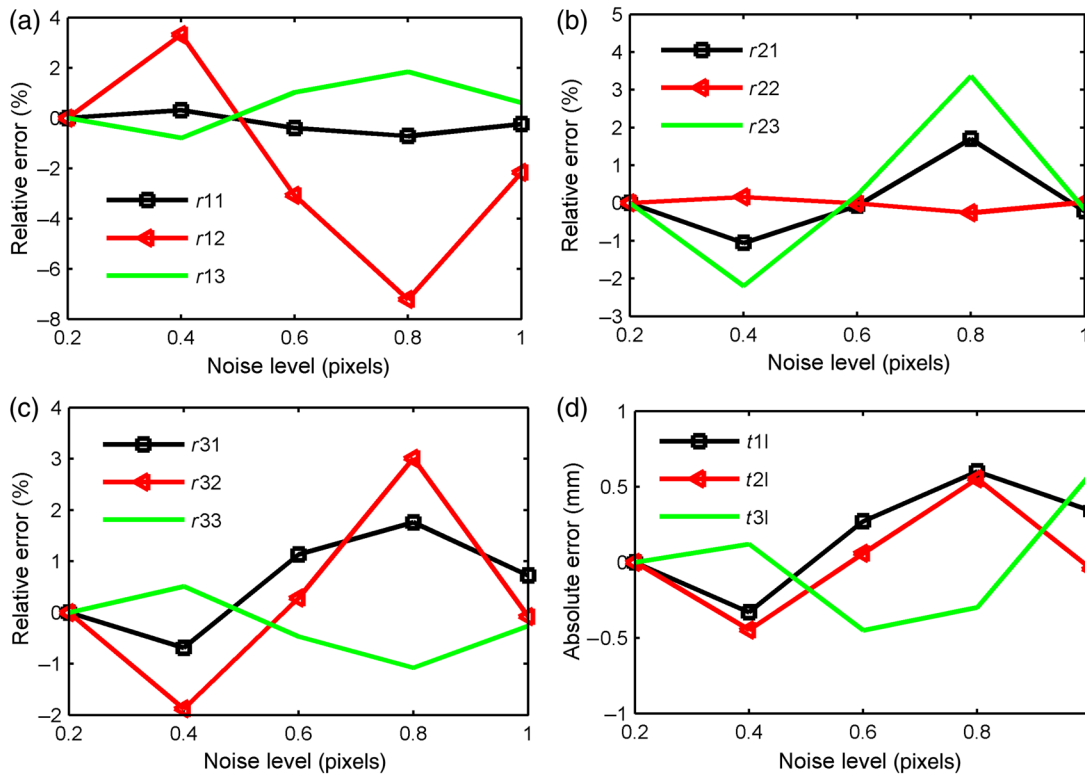


Fig. 4 Effects of pixel coordinates noise on calibration accuracy of the external parameters with an analytical method in Sec. 3.2: (a)–(c) the elements in the rotation matrix R ; (d) the elements in the translation vector T .

also be applied to improve accuracy next. To sum up, the iterative refinement process is mainly composed of two steps:

1. Refine left and right camera parameters, respectively: project the feature point M_{wj} to image plane with a pure perspective projection relationship. Compute the distorted image point \bar{m}_{uj} (j represents the j 'th point) from the ideal point according to Eq. (6). Construct the objective function that minimizes the discrepancy between the calculated image point \bar{m}_{uj} and the

detected image point m_{uj} . At each iteration, the intrinsic, external parameters and distortion coefficients are chosen as variables.

2. The A_l, A_r , and (R_l, T_l) have been obtained in step (1); in this step, we employ Levenberg–Marquardt algorithm to the optimization of the structure parameters (R, T) . According to the collinear geometry, M_{wj} , \bar{m}_{1lj} , and \bar{m}_{1rj} lie in the same line. Then, we calculate the object point with the collinear geometry, denoted as \hat{M}_{wj} . Construct the objective function that minimizes the difference between the calculated object point \hat{M}_{wj} and the true value M_{wj} under 3-D measurement coordinate system. In this way, the error criterion during the optimization process is in accordance with that during vision measurement process.

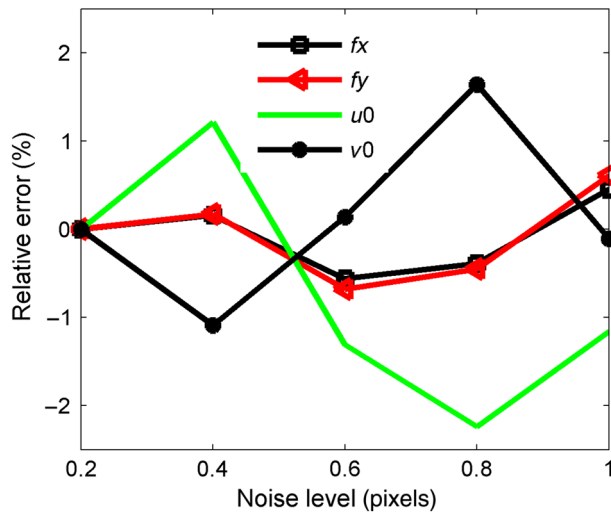


Fig. 5 Effects of pixel coordinates noise on calibration accuracy of the internal parameters with an analytical method in Sec. 3.2.

4 Experimental Results

4.1 Computer Simulation

For the simulated binocular system, either of the simulated camera's image size is 2456×2058 pixels with the principal point at $(u_0, v_0) = (1228, 1029)$ pixel. The skew factor is set to zero. The distortion center is the same as the principal point for simplification. The model plane is a checkerboard target with 54 corners (9×6) uniformly distributed, and the minimum point interval is 30 mm. The reference word coordinate system is built on the target, and the Z axis is perpendicular to the target. The rotation vector and translation vector of the structure parameters are fixed as $r = [0.1 \text{ deg},$

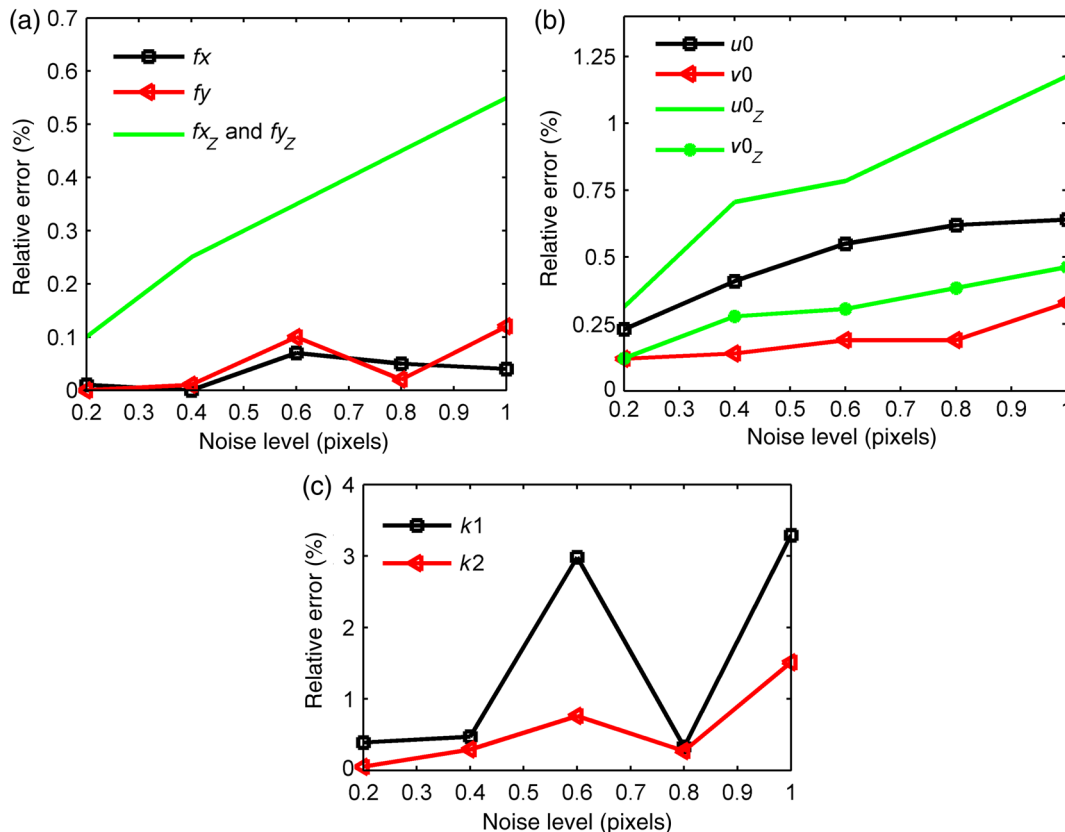


Fig. 6 Effects of pixel coordinates noise on calibration accuracy with maximum likelihood estimation method: (a) focal length f_x and f_y , (b) principal point, (c) distortion coefficients.

0.1 deg, 0.2 deg] and $T = [80, 0, 0]$. The orientation and the translation between the world coordinate system and the left camera are set as follows: object-to-camera distance is 400 to 800 mm and the angle between the target plane and the image plane is 30 deg to 70 deg. Gaussian noise of mean 0 and standard deviations ranged from 0 pixel to 1 pixel is added to coordinates of the images.

Figures 4 and 5 show the influence of noise on the relative errors of intrinsic and structure parameters with an analytical method in Sec. 3.1. The result is only the average result of three times. In this part, we calculate the intrinsic and structure parameters with only 12 point pairs. All the curves change greatly and the vibrates range tends to be larger with higher noise level. This phenomenon can be explained as that too few points are selected.

Figures 6 and 7 show the influence of noise on the relative errors after refinement. The internal parameters calibration result is compared with Zhang⁶ (the curve of f_{y_z} , f_{x_z} , $u0_z$, and $v0_z$). It is noticeable that our method is better than Zhang and produces smooth result in most cases than an analytical



Fig. 9 The binocular vision system to be calibrated.

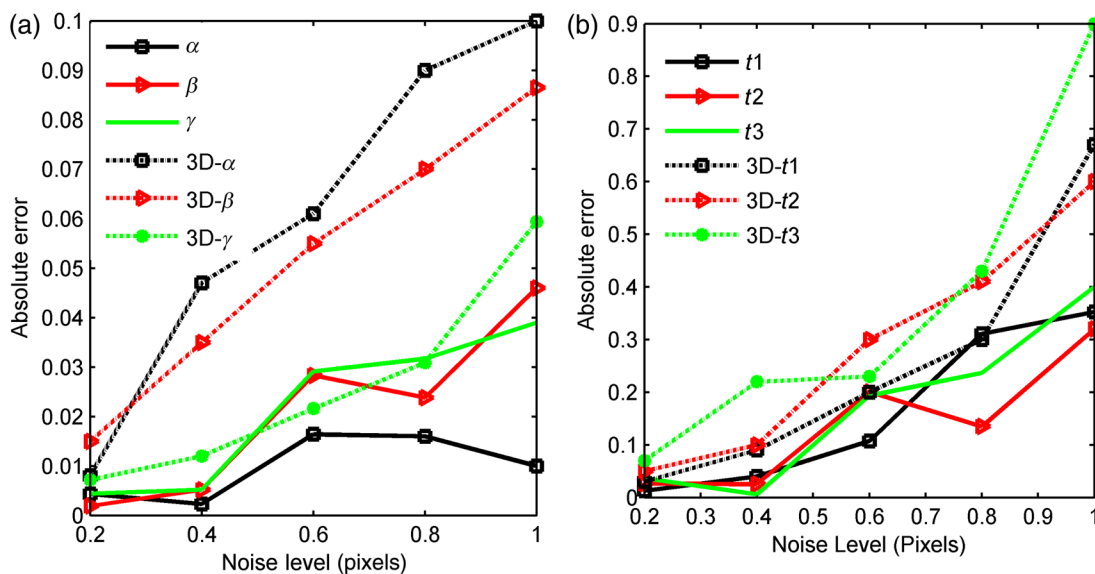


Fig. 7 Effects of pixel coordinates noise on calibration accuracy with maximum likelihood estimation method, and the curves of variables marked with 3-D are results of Ref. 4, the others are results of our method: (a) the rotation angles between the right and the left cameras and (b) the translation vector between the right and the left cameras.

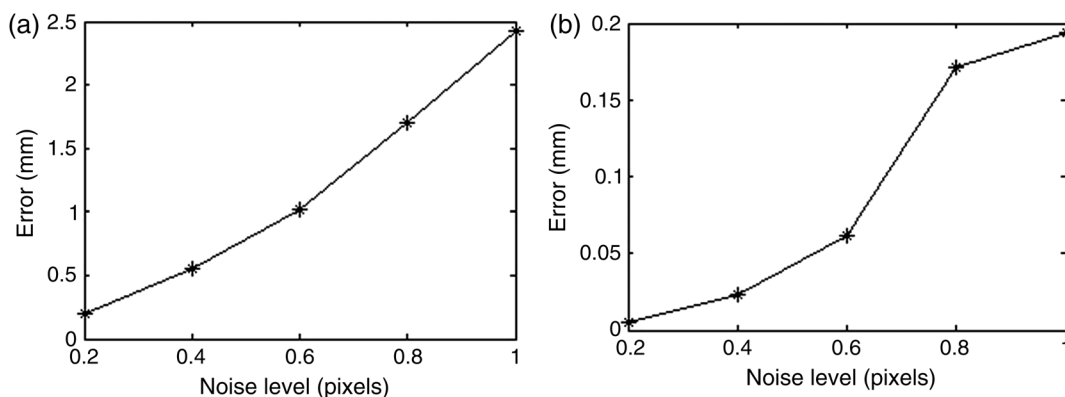


Fig. 8 Effects of pixel coordinates noise on calibration accuracy: (a) the y axis represents the value of ERMS and (b) the y axis represents the value of ED-D [Eq. (19)].



Fig. 10 Accuracy verification experiment of the calibration method.

method. The structure parameters calibration result is compared with the 3-D method in Ref. 4. As we can see, the absolute errors of the rotation vector R and the translation vector T are reduced greatly after optimization and they increase almost linearly with the noise level.

In addition, it is necessary to define suitable error criteria for evaluating accuracy in terms of camera parameters. Two error criteria are selected to evaluate the calibration accuracy: the accuracy of calibration and the 3-D measurement are evaluated.^{11,19} Using synthetic data generated with known camera parameters, it is easy to calculate the averaged Euclidean distance between the given global coordinates M and the reconstructed global coordinate \bar{M} . This is a criterion for evaluating accuracy in terms of camera parameters denoted as ERMS (the root mean square). The other error criterion is defined to evaluate the astringency of the calibration method with D -value of two distances, one is the distance between noise affected coordinates M and the real coordinates \bar{M} , and the other is the distance between noise affected coordinates and the reconstructed global coordinate $\bar{\bar{M}}$. This error criterion is represented as Eq. (19). Figure 8 displays the two error criterions with respect to different noise levels

$$E_{D-D} = \frac{1}{n} \left[\sum_{i=1}^N \|M - \bar{M}(A, K, R, T)\|^2 - \sum_{i=1}^N \|M - \bar{M}(\bar{A}, \bar{K}, \bar{R}, \bar{T})\|^2 \right]. \tag{19}$$

Table 1 Calibration results of the global optimization.

	Left camera	Right camera
Focal length (f_x, f_y)	(2654.01486, 2653.99860)	(2659.58722, 2660.14685)
Principle point (u_0, v_0)	(939.44415, 317.11301)	(898.47397, 407.47303)
Distortion coefficient (k_1, k_2)	(−0.10938, −0.00139)	(−0.10259, −0.00142)
Translation vector (t_1, t_2, t_3)	(−183.83186, 1.42684, 39.44175)	
Rotation vector	(0.00166, 0.42276, −0.00790)	

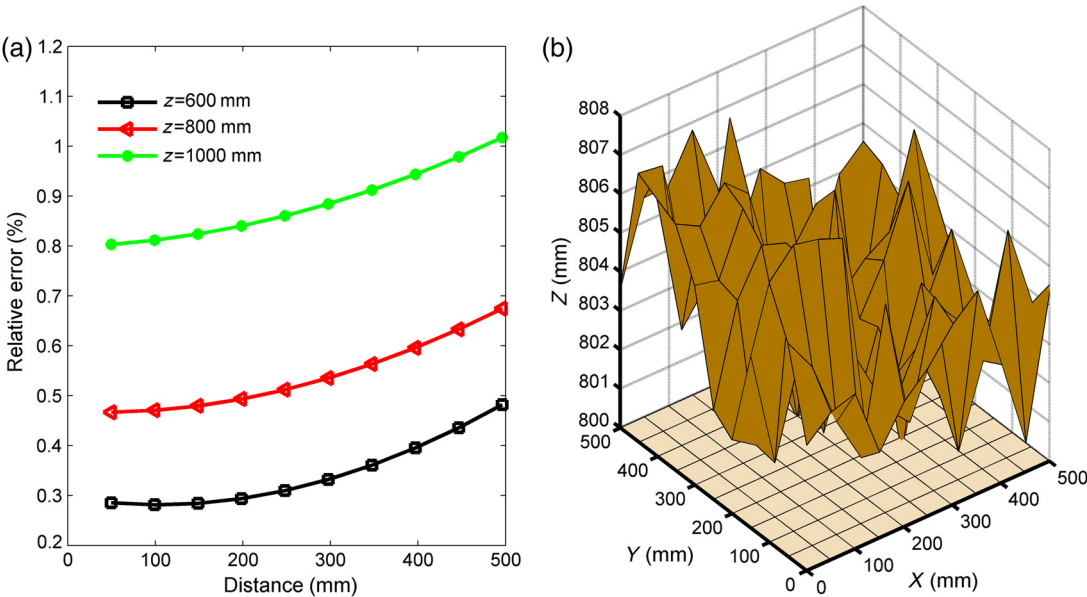


Fig. 11 The accuracy of the proposed calibration method: (a) the average reconstruction errors with different distances and (b) the reconstructed target plane in 800 mm.

4.2 Real Data

To evaluate the accuracy of the proposed calibration method, accuracy evaluation experiments are conducted. The experimental system is shown in Fig. 9, consisting of two monochrome CCD cameras (the middle two cameras), with a resolution of 2456×2058 pixels and a pixel size of $6.5 \mu\text{m}$. The target is shown in Fig. 10 and its size is $500 \text{ mm} \times 500 \text{ mm}$. The images of the targets are captured by the binocular system randomly, which are in the range of the following position parameters: object-to-camera distance is 600 to 1000 mm. We choose the library function provided by OPENCV to extract corners of the target and determined the correspondence in the binocular imaging. The experiments consist of two parts. The system is calibrated with our method first, and the calibration results are shown in Table 1. Next, the calibration accuracy is analyzed. 3-D coordinates of the feature points in target are reconstructed and the average reconstruction error is calculated as shown in Fig. 11(a). The reconstructed target plane in 800 mm is shown in Fig. 11(b).

5 Conclusion

In this paper, a noniterative and effective camera calibration method is proposed. The noniterative method overcomes many problems with the conventional iterative approach. Moreover, only one image pair is needed to solve the binocular system parameters. For the refinement of structure parameters, the objective function is established by minimizing metric distance between the reconstructed point and the real point in 3-D space. In this case, the error criterion during the optimization process is in accordance with that during the subsequent measurement process. This is more persuasive than the traditional 2-D method. The reconstructed point is calculated by the collinear geometry. Experiments on synthetic and real data have been compared with the conventional method. When the standard division of the noise is smaller than 1 pixel, the relative errors of internal camera parameters are smaller than 1.25% and the absolute errors of structure parameters are smaller than 0.045 deg or 0.4 mm . The result demonstrates the advantage of this approach. This proposed calibration method can be used in both single camera and binocular system calibration. The whole calibration procedure is easily constructed without any special requirement.

Acknowledgments

I would particularly like to thank my workmate, who has suggested numerous improvements to both the content and presentation of this paper and whose own work on feature point extraction has contributed to this approach. This work was supported by the National Natural Science Foundation of China (NSFC) under Grants Nos. 11074152 and 10934003.

References

1. S. Zhu and Y. Gao, "Noncontact 3-D coordinate measurement of cross-cutting feature points on the surface of a large-scale workpiece based on the machine vision method," *IEEE Trans. Instrum. Meas.* **59**(7), 1874–1887 (2010).
2. W. Wang, J. G. Zhu, and J. R. Lin, "Calibration of a stereoscopic system without traditional distortion models," *Opt. Eng.* **52**(9), 093104 (2013).
3. M. Machacek, M. Sauter, and T. Rosgen, "Two-step calibration of a stereo camera system for measurements in large volumes," *Meas. Sci. Technol.* **14**(9), 1631–1639 (2003).
4. Y. Cui et al., "Precise calibration of binocular vision system used for vision measurement," *Opt. Express* **22**(8), 9134–9149 (2014).
5. Z. Z. Wei and X. K. Liu, "Vanishing feature constraints calibration method for binocular vision sensor," *Opt. Express* **23**(15), 18897–19814 (2015).
6. Z. Y. Zhang, "A flexible new technique for camera calibration," *IEEE Trans. Pattern Anal. Mach. Intell.* **22**(11), 1330–1334 (2000).
7. S. J. Maybank and O. D. Faugeras, "A theory of self-calibration of a moving camera," *Comput. Vision* **8**(2), 123–151 (1992).
8. R. Y. Tsai, "A versatile camera calibration technique for high-accuracy 3D machine vision metrology using off-the-shelf TV cameras and lenses," *IEEE J. Rob. Autom.* **3**(4), 323–344 (1987).
9. J. Y. Weng, P. Cohen, and M. Herniou, "Camera calibration with distortion models and accuracy evaluation," *IEEE Trans. Pattern Anal. Mach. Intell.* **14**(10), 965–980 (1992).
10. R. I. Hartley, "Self-calibration of stationary cameras," *Comput. Vision* **22**(1), 5–23 (1997).
11. Z. Jia et al., "Improved camera calibration method based on perpendicularity compensation for binocular stereo vision measurement system," *Opt. Express* **23**(12), 15205–15223 (2015).
12. F. Y. Imaztirk, "Full-automatic self-calibration of color digital cameras using color targets," *Opt. Express* **19**(19), 18164–18174 (2011).
13. S. D. Ma, "A self-calibration technique for active vision systems," *IEEE Trans. Rob. Autom.* **12**(1), 114–120 (1996).
14. F. C. M. Alanís and J. A. M. Rodríguez, "Self-calibration of vision parameters via genetic algorithms with simulated binary crossover and laser line projection," *Opt. Eng.* **54**(5), 053115 (2015).
15. J. A. M. Rodríguez, "Binocular self-calibration performed via adaptive genetic algorithm based on laser line imaging," *Mod. Opt.* **63**(13), 1219–1232 (2016).
16. J. Apolinar and M. Rodríguez, "Three-dimensional microscope vision system based on micro laser line scanning and adaptive genetic algorithms," *Opt. Commun.* **385**, 1–8 (2017).
17. M. Vo et al., "Advanced geometric camera calibration for machine vision," *Opt. Eng.* **50**(11), 110503 (2011).
18. Y. Z. Hong, G. Q. Ren, and E. H. Liu, "Non-iterative method for camera calibration," *Opt. Express* **23**(28), 23992–24003 (2015).
19. J. Apolinar and M. Rodríguez, "Online self-calibration for mobile vision based on laser imaging and computer algorithms," *Opt. Lasers Eng.* **49**(6), 680–692 (2011).

Enkun Cui received his BS and MS degrees in physics from Lanzhou University in 2012 and his MS degree from the University of Chinese Academy of Sciences in 2014. He is working on his PhD in engineering with specialization in optics at the University of Chinese Academy of Sciences. His current research interests include machine vision and digital image processing.

YanJie Wang received his BS degree from Jilin University of Technology in 1988 and his MS degree in 1998 from Changchun Institute of Optic, Fine Mechanics and Physics (CIOMP). Now, he is a professor at CIOMP. His research interests are focused on laser and photoelectric measuring technology, such as target recognition, attitude measurement, machine vision, and large-scale precision metrology.

Tao Zhang received his BS degree from Zhejiang University in 1987. Now, he is a professor at CIOMP. His research interests are focused on detection and imaging technology and control technique.

Nan Di received her PhD from the Chinese Academy of Sciences in 2007. Currently, she is a researcher at CIOMP. Her research interests are focused on vision measurement and photoelectric measuring technology.

YanHe Yin is working on his PhD in engineering with specialization in optics at the University of Chinese Academy of Sciences. His research interest is focused on optical design.

Pei Wu received his PhD from the Chinese Academy of Sciences in 2017. His research interest is focused on digital image processing and program.

HongHai Sun received his PhD from the Chinese Academy of Sciences in 2008. Currently, he is a researcher at CIOMP. His research interests are focused on vision measurement and photoelectric measuring technology.